known to control differentiation of root hair cells (*21*, *22*), the cell type infected by *Rhizobium*. Thus, endogenous ethylene may affect the persistence of rhizobial infection by controlling the formation of infectable root hair cells. Alternatively, ethylene may act as a diffusible signal for activation of mechanisms that arrest rhizobial infection. ACC is inhibitory to nodulation when applied after the initiation of rhizobial infection (Fig. 5A, 24 and 48 hours). Similarly, the ethylene biosynthesis inhibitor AVG can increase nodule number when applied after the initiation of infection (*5*). These observations are consistent with a model wherein endogenous ethylene acts subsequent to infection initiation and root hair differentiation.

If ethylene provides a signal for induction of infection arrest, then plant cells containing persistent *Rhizobium* infections either must avoid the ethylene signal or must be insensitive to the signal. Localized production of ethylene at sites of infection arrest could facilitate avoidance of ethylene by infections destined for nodule colonization. A model for cell-specific regulation of ethylene synthesis during root hair cell differentiation has been proposed in *Arabidopsis* (*22*). In wild-type *M. truncatula*, all rhizobial infections can be blocked by treatment with ACC as late as 48 hours after inoculation (Fig. 5A), indicating that infections destined for nodule colonization are not inherently insensitive to ethylene. However, after macroscopic nodule primordia appear, nodulation is largely insensitive to exogenous ACC (Fig. 5A, 72 hours); thus, sustained rhizobial infections may acquire insensitivity to ethylene.

In plant-pathogen interactions, ethylene has been implicated as an endogenous cue for induction of host defense-related genes (*23*). Despite extensive correlative data, however, a causal role for ethylene in resistance to pathogens has not been established (*24*). In *M. truncatula*, the *sickle* mutation causes extensive developmental abnormalities and hyperinfection by *Rhizobium*, which indicates that *skl1* encodes a function common to both plant development and control of rhizobial infection.

REFERENCES AND NOTES

1. T. Bhuvaneswari, A. A. Bhagwat, W. D. Bauer, *Plant Physiol.* **68**, 1144 (1981); G. Caetano-Anolles and W. D. Bauer, *Planta* **175**, 546 (1988); G. Caetano-Anolles and P. M. Gresshoff, *J. Plant Physiol.* **138**, 765 (1991).
2. B. J. Carroll, D. L. McNeil, P. M. Gresshoff, *Plant Physiol.* **78**, 34 (1985); *Proc. Natl. Acad. Sci. U.S.A.* **82**, 4162 (1985).
3. J. Vasse, F. de Billy, G. Truchet, *Plant J.* **4**, 555 (1993).
4. K. Niehaus, D. Kapp, A. Puhler, *Planta* **190**, 415 (1993); S. Perotto, N. J. Brewin, E. L. Kannenberg, *Mol. Plant-Microbe Interact.* **7**, 99 (1994).
5. N. K. Peters and D. K. Crist-Estes, *Plant Physiol.* **91**, 690 (1989).
6. J. C. Fearn and T. A. LaRue, *ibid.* **96**, 239 (1991); F. C. Guinel and T. A. LaRue, *ibid.* **97**, 1206 (1991); *ibid.* **99**, 515 (1992).
7. X. Ruan and N. K. Peters, *J. Bacteriol.* **174**, 3467 (1992).
8. K. H. Lee and T. A. LaRue, *Plant Physiol.* **100**, 1759 (1992).
9. F. Ligero *et al.*, *ibid.* **97**, 1221 (1991); K. H. Lee and T. A. LaRue, *ibid.* **100**, 1334 (1992).
10. R. V. Penmetsa and D. R. Cook, in preparation.
11. S. A. Leong, P. H. Williams, G. S. Ditta, *Nucleic Acids Res.* **13**, 5965 (1985).
12. C. Boivin *et al.*, *Plant Cell* **2**, 1157 (1990). X-Gal is 5-bromo-4-chloro-3-indolyl-β-D-galactopyranoside.
13. Infections and nodule primordia are first evident on wild-type and *sickle* roots by 36 to 48 hours after inoculation. However, nodule development is retarded in *sickle*, such that 21-day-old nodules are about one-tenth the size of wild-type nodules of similar age.
14. M. B. Lanahan *et al.*, *Plant Cell* **6**, 521 (1994).
15. J. R. Ecker, *Science* **268**, 667 (1995).
16. L. I. Knight, R. C. Rose, W. Crocker, *ibid.* **31**, 635 (1910); P. Guzman and J. R. Ecker, *Plant Cell* **2**, 513 (1990).
17. A. B. Bleecker, M. A. Estelle, C. Somerville, H. Kende, *Science* **241**, 1086 (1988).
18. J. Hua, C. Chang, Q. Sun, E. M. Meyerowitz, *ibid.* **269**, 1712 (1995); C. Chang and E. M. Meyerowitz, *Proc. Natl. Acad. Sci. U.S.A.* **92**, 4129 (1995).
19. G. Roman *et al.*, *Genetics* **139**, 1393 (1995).
20. Isolated leaves were floated on water and treated with ethylene (100 ppm) (*17*). After 5 days dark incubation at 21°C, leaves of wild-type and *sickle* controls were chlorotic and green, respectively.
21. J. D. Masucci and J. W. Schiefelbein, *Plant Cell* **8**, 1505 (1996); *Plant Physiol.* **106**, 1335 (1994).
22. M. Tanimoto, K. Roberts, L. Dolan, *Plant J.* **8**, 943 (1995).
23. J. R. Ecker and R. W. Davis, *Proc. Natl. Acad. Sci. U.S.A.* **84**, 5202 (1987); F. Mauch, J. B. Meehl, A. J. Staehelin, *Planta* **186**, 367 (1992).
24. A. F. Bent *et al.*, *Mol. Plant-Microbe Interact.* **5**, 372 (1992); P. Silverman *et al.*, *ibid.* **6**, 775 (1993); K. Lawton *et al.*, *ibid.* **8**, 863 (1995).
25. F. deBilly *et al.*, *Plant J.* **1**, 27 (1991).
26. N. Chaubet, B. Clement, C. Gigot, *J. Mol. Biol.* **225**, 569 (1992).
27. P. Somasegaran and H. J. Hoben, *Handbook for Rhizobia: Methods in Legume-Rhizobium Technology* (Springer-Verlag, New York, 1994), pp. 392–398.

28. Supported by grants from the NSF Program on Integrative Plant Biology (IBN-9507535) and from the Samuel Roberts Noble Foundation.

15 July 1996; accepted 2 December 1996

Measuring Serotonin Distribution in Live Cells with Three-Photon Excitation

S. Maiti, Jason B. Shear,* R. M. Williams, W. R. Zipfel, Watt W. Webb†

Tryptophan and serotonin were imaged with infrared illumination by three-photon excitation (3PE) of their native ultraviolet (UV) fluorescence. This technique, established by 3PE cross section measurements of tryptophan and the monoamines serotonin and dopamine, circumvents the limitations imposed by photodamage, scattering, and indiscriminate background encountered in other UV microscopies. Three-dimensionally resolved images are presented along with measurements of the serotonin concentration (~50 mM) and content (up to ~5×10^8 molecules) of individual secretory granules.

Neurotransmitter granules have typically been studied either with various imaging techniques (*1*, *2*) that do not directly detect the granular content, or with chemical or electrical assays (*3*, *4*) that identify the granule contents but can probe only the extracellular medium. Thus, it has not been possible to determine neurotransmitter concentration or total neurotransmitter content of individual granules in intact cells. As a solution, we have excited the native UV fluorescence of these molecules by simultaneous absorption of three infrared photons, which accesses shorter wavelength UV transitions in living cells than conventional or two-photon microscopy (*5*).

When subjected to a high-intensity irradiation at wavelength λ, a molecule that ordinarily absorbs at λ/3 may exhibit fluorescence at ≳λ/3 by a three-photon absorption mechanism (*6*). The average fluorescence photon count rate F measured from three-photon excitation depends on the three-photon molecular absorption cross section σ_3 [unit: (length)^6 (time)^2 (photon)$^{-2}$], the instantaneous intensity I, the fluorescence quantum efficiency Q, the detection efficiency K, the wavelength λ, and the concentration C (number of molecules per unit volume). Analogous with two-photon excitation (*7*), F is determined by the product of I^3 and C, integrated over space (**r**) and time (t'):

$$F = KQ\sigma_3[(1/\Delta t)\int_0^{\Delta t}\int_0^{\infty} I^3(\mathbf{r},t')C(\mathbf{r},t')\,d\mathbf{r}\,dt'] \quad (1)$$

For excitation of a homogeneous dye solution with a focused and pulsed laser beam with a gaussian temporal and spatial profile, the integral yields (SI units)

School of Applied and Engineering Physics, Cornell University, Ithaca, NY 14853, USA.

All authors contributed equally to this work.
*Present address: Department of Chemistry and Biochemistry, University of Texas, Austin, TX 78712, USA.
†To whom correspondence should be addressed.

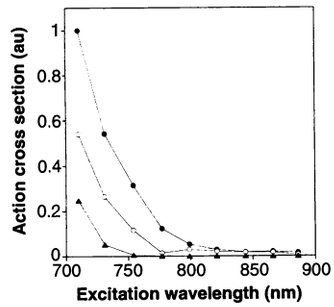

Fig. 1. Three-photon absorption spectra of Trp (open circles, values multiplied by 2), serotonin (filled circles), and dopamine (filled triangles, values multiplied by 4) (*17*). Relative errors in the data are <10% of the respective values. The absolute value of the three-photon fluorescence action cross section ($Q\sigma_3$, see Eq. 2) for Trp at 710 nm is estimated to be 2×10^{-96} m^6 s^2 photon^{-2}, which can be used as a scaling factor for the graph. Because of uncertainties involved in estimating the collection efficiency (K in Eq. 2), the absolute value has a large uncertainty (~5×); au, arbitrary unit.

$$F = (4.3 \times 10^{73}) \times [QKCP_{av}{}^3(\lambda/\omega_0)^2\sigma_3]/[f^2\tau^2] \quad (2)$$

where P_{av} is the average power, f is the pulse repetition rate of the laser, τ is the full-width-at-half-maximum (FWHM) pulsewidth, and ω_0 is the beam waist (radius of the $1/e^2$ intensity contour at the focal plane). This expression reveals the importance of minimizing the focused beam waist and reducing the pulsewidth for maximizing the fluorescence at a given average excitation power. Because λ/ω_0 is nearly independent of λ for a focused Gaussian beam, a measurement of F as a function of λ yields the dependence of σ_3 on λ. The results of such measurements for tryptophan (Trp), serotonin, and dopamine between 710 and 886 nm are shown in Fig. 1. The shape of the three-photon excitation (3PE) spectrum of Trp differs from the linear (one photon, σ_1) spectrum (*8*). For example, $\sigma_{1(270\ nm)}:\sigma_{1(237\ nm)} = 1:5$, whereas in the measured three-photon spectrum the corresponding ratio is $\sigma_{3(810\ nm)}:\sigma_{3(710\ nm)} = 1:30$. For each species, the fluorescence count rate at low powers (5 to 25 mW) shows a cubic dependence on excitation power (*9*), as expected for 3PE (Eq. 2).

These cross section measurements show how 3PE fluorescence can be used to image the distribution of proteins and neurotransmitters in cellular environments at reasonably benign laser intensities. We built a three-photon UV fluorescence microscopy apparatus based on an existing laser-scanning microscope capable of imaging with two- (*5*) or three-photon (*10*) excitation of visible emission dyes. We collected 3PE UV fluorescence images of rat basophilic leukemia (RBL-2H3) cells that were incubated in 250 μM serotonin for 6 hours. Serotonin is actively transported into these cells, and subsequently into secretory granules. It is released in response to immunogenic stimulation by substances in the extracellular environment (*11*). The images contain sets of ~20 different horizontal planes ("optical slices") through the cell bodies in increments of 1.3 μm. A 3PE fluorescence image of a single optical slice 3 μm above the cover slip is shown in Fig. 2A. The corresponding intrinsic fluorescence image from a control culture of cells that lacked serotonin in the incubation medium is shown in Fig. 2B. Bright punctate features are evident only in the cells that were loaded with serotonin. The spectral characteristics of the punctate fluorescence and its absence in the control cells indicate that the fluorescence is generated by serotonin (or potentially a serotonin metabolite) sequestered in granules. Substantial (~75%) disappearance of the punctate features after immunogenic stimulation was also observed (*9*) and supports this conclusion. The observed granules may represent both individual vesicles and vesicular clusters that are not separately resolved in the image (*12*). Figure 3 shows the front and the top view of a three-dimensionally reconstructed image obtained from a set of serotonin-loaded RBL cells (*13*). The three-dimensional image contains the information required to calculate the volume of each of the observed serotonin granules. Such measurements performed with ~400 cells yielded a volume distribution histogram (Fig. 4) for these granules (*14*).

Calibration of the granular fluorescence with solutions of known concentrations yields a value of ~50 mM for the concentration of serotonin in the larger (>1-μm diameter) granules (*15*). The concentration calibration, together with our volume measurements, provides a measure of the total serotonin content of individual granules or cells. For example, the largest 5% of the granules have an

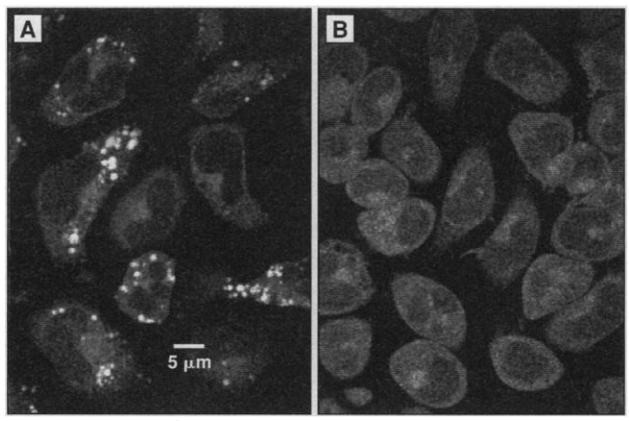

Fig. 2. Images of RBL cells obtained from 3PE fluorescence of serotonin and other cellular components (*18*). (**A**) Cells incubated in 250 μM serotonin for 6 hours (imaged at a horizontal focal plane 3 μm above the cover slip.) (**B**) Control cells without serotonin incubation. Punctate fluorescence in (A) is caused by serotonin granules.

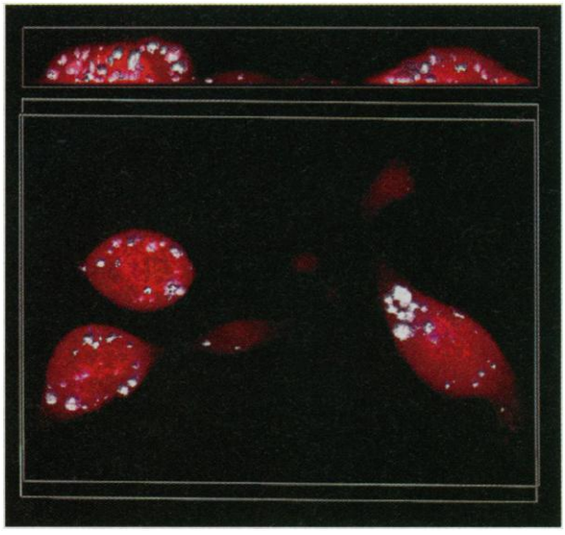

Fig. 3. Three-dimensional image of a set of serotonin-loaded RBL cells. The excitation wavelength was 700 nm, and the average power at the sample ~25 mW. The image is rendered by reconstruction of 20 optical slices. This reconstruction draws isointensity surfaces (white) around regions of equal or higher brightness to demarcate the granules. The red hue represents intensity below the granular cutoff intensity, and thus the density of red overlapping an object provides a depth cue. Box width is 80 μm.

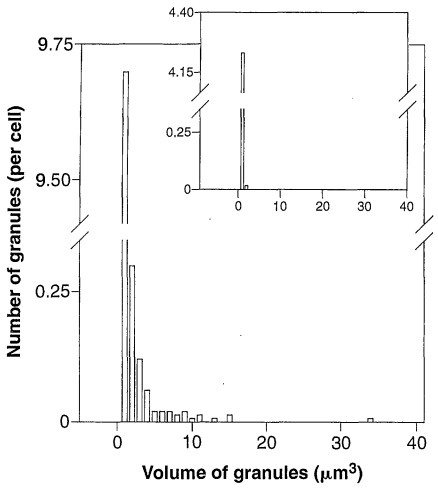

Fig. 4. Histograms of the distribution of granule volume. Cells were incubated in serotonin for 6 hours. (**Inset**) Histogram obtained from control cells. The histograms represent the average distributions obtained from ~400 randomly chosen cells. Serotonin-incubated cells can have 0 to ~20 recognizable serotonin granules per cell, with a wide variability observed even among neighboring cells. The small (0 to 1 μm^3) granules counted in control cells indicate the level of background in these measurements.

average volume of 4 μm^3 (Fig. 4) and thus contain, on average, $\sim 10^8$ serotonin molecules per granule.

Three-photon excitation thus enables quantitative imaging of cellular processes by harnessing the UV fluorescence of native molecules. This technique offers a necessary complement to extracellular secretion assays such as carbon-fiber amperometry (4), providing the ability to measure the distribution and content of neurotransmitter granules within viable cells.

Note added in proof: We have recently learned that Tan *et al.* (16) have reported qualitative detection of a general brightness increase of astrocytes incubated in serotonin.

REFERENCES AND NOTES

1. K. Miyake and P. L. McNeil, *J. Cell Biol.* **131**, 1737 (1995); T. A. Ryan, S. J. Smith, H. Reuter, *Proc. Natl. Acad. Sci. U.S.A.* **93**, 5567 (1996).
2. A. Spudich and D. Braunstein, *Proc. Natl. Acad. Sci. U.S.A.* **92**, 6976 (1995).
3. M. A. De Matties, C. De Tullio, R. Buccione, A. Luini, *J. Biol. Chem.* **266**, 10452 (1991); D. M. Phillips, P. Bashkin, I. Pecht, *J. Ultrastruct. Res.* **90**, 105 (1985); H. Tamir, T. C. Theoharides, M. D. Gershon, P. W. Askenase, *J. Cell Biol.* **93**, 638 (1982).
4. P. A. Garris and R. M. Wightman, *J. Physiol.*, **478**, 239 (1994); D. Bruns and R. Jahn, *Nature* **377**, 62 (1995); R. H. Chow *et al.*, *ibid.* **356**, 60 (1992); G. Liu and R. W. Tsien, *Neuropharmacology* **34**, 1407 (1995); S. Zerby and A. Ewing, *Brain Res.* **712**, 1 (1996).
5. W. Denk, J. H. Stricker, W. W. Webb, *Science* **248**, 73 (1990); R. M. Williams, D. W. Piston, W. W. Webb, *FASEB J.* **8**, 804 (1994).
6. S. Singh and L. T. Bradley, *Phys. Rev. Lett.* **12**, 612 (1964).
7. C. Xu and W. W. Webb, *J. Opt. Soc. Am. B* **13**, 481 (1996).
8. F. W. J. Teale and G. Weber, *Biochemistry* **65**, 476 (1957).
9. S. Maiti, J. B. Shear, R. M. Williams, W. R. Zipfel, W. W. Webb, data not shown.
10. C. Xu *et al.*, *Proc. Natl. Acad. Sci. U.S.A.* **93**, 10763 (1996).
11. S.-Y. Mao *et al.*, *Biochemistry* **34**, 1968 (1995), and references therein; J. S. Bonifacino, L. Yuan, I. S. Sandoval, *J. Cell Sci.* **92**, 701 (1989); see J. M. Oliver *et al.*, *Prog. Allergy* **42**, 185 (1988), for a review.
12. The cellular background fluorescence, present both in serotonin-loaded and control cells, maps the distribution of Trp-containing proteins (and possibly other cellular material possessing similar spectral characteristics) in these cells. The nuclei, which presumably contain a lower concentration of such molecules, are seen as darker regions.
13. The cells remain capable of exocytosis after exposure to the infrared radiation used in generating a three-dimensional image (9). In contrast, we have thus far been unable to observe exocytosis after exposure to 450-nm radiation required for two-photon excited fluorescence imaging of the granules, indicating the presence of possible wavelength-dependent photochemical mechanisms that make 3PE less damaging. Infrared illumination caused some visible (>400 nm) wavelength fluorescence from the serotonin granules. Whether this originates from indolic degradation products suggested in the literature [C. Lambert *et al.*, *Biochim. Biophys. Acta* **993**, 12 (1989)] is currently under investigation (J. B. Shear, C. Xu, R. M. Williams, S. Maiti, W. W. Webb, unpublished data).
14. To obtain the volume distribution histogram, we first identified granules by calculating isointensity surfaces at a pixel intensity of $I_0 + 7\sigma$, where I_0 and σ are the mean and standard deviation of the pixel intensity obtained from the control cells. A relatively high cutoff intensity was chosen to distinguish the brightest granules. Changing the cutoff intensity to $I_0 + 8.5\sigma$ would result in <50% decrease in the number of granules. The program (Data Explorer, IBM) used for the calculation interpolates between pixel values to locate the position of the isosurfaces. Subsets of the overall isosurface that represent individual granules were obtained by a sorting algorithm that identifies disconnected isointensity regions. For each isosurface subset, we obtain a set of polygons (with area A_i) that represent its intersection with a series of N horizontal planes spaced along the vertical (z) direction. Granule volume (V) is then calculated as
$$V = [\Delta z/(N - 1)]\Sigma(A_i) \quad (3)$$
where Δz is the extent of the granule along the z direction and the sum is taken over all horizontal planes intersected by the granule.
15. We have measured fluorescence as a function of serotonin concentration (from solutions buffered at ~pH 6) under conditions identical to imaging. The fluorescence increases approximately linearly at lower (≲50 mM) concentrations, but the slope decreases at higher concentrations {presumably as a result of quenching by energy transfer to neighboring molecules [T. Förster, *Ann. Phys. (Leipzig)* **2**, 55 (1948), translated by R. S. Knox, University of Rochester]}. The intensity peaks at ~250 mM and decreases thereafter. A priori, the observed level of granular fluorescence may also represent a concentration in this "inverted" region, but a time-dependent study of serotonin loading in these cells (9) rules out this possibility. Also, serotonin fluorescence is pH-sensitive, and the vesicle interiors are believed to be acidic [M. B. De Young *et al.*, *Arch. Biochem. Biophys.* **254** 222 (1987)]. We infer from measurements of fluorescence as a function of pH (9) that our estimate (made at pH 6) should be accurate to ±25% for vesicular pH between 5 and 7. Nevertheless, unknown factors in the vesicle lumen may introduce larger errors.
16. W. Tan *et al.*, *Anal. Chem.* **67**, 2575 (1995).
17. Serotonin, dopamine, and Trp were obtained from Sigma (certified >99% pure by thin-layer chromatography) and used without further purification. Samples at 5 mM concentration were prepared in 25 mM Mops buffer (pH 7.0) and measured at room temperature with excitation by a mode-locked 76-MHz titanium:sapphire laser source (MIRA 900, Coherent). The laser beam was passed through a Pockel's cell–based noise controller (LASS II, Conoptics) and a longpass dichroic reflector (400 DCLP, Omega) and finally focused into the sample by a microscope objective [1.25 numerical aperture (NA), oil immersion, Zeiss Neofluar]. The sample was contained in a 0.9 mm by 0.9 mm square glass capillary tube (number 8290, VitroDynamics; uniform transmission between 300 and 700 nm) with 170-μm-thick walls. The UV fluorescence was collected by the same objective and reflected by the UV dichroic onto a Hamamatsu HC125-02 photon-counting module, after passing through a series of UV bandpass filters (UG11 colored glass filter from Schott and interference filters from Corion). The output of the detector was transmitted to a Stanford Research Systems SR400 photon counter, which provided the fluorescence count rate. The pulsewidth at each wavelength (160 to 220 fs) was measured by an intensity autocorrelator (FR103, Femtochrome), and the average power was measured by a thermopile power meter (Molectron).
18. Excitation was by an 80-MHz mode-locked titanium: sapphire laser (Tsunami, Spectra-Physics), with λ = 700 nm, $P_{av} \sim 25$ mW, $\tau \sim 100$ fs, and the exposure time required to collect the image of a single plane was ~1 s. The excitation beam overfilled the back aperture of the objective. Occasionally cell damage was observed during imaging at this power and wavelength, but it could be minimized by excitation at 740 nm. Images were smoothed by 5 × 5 Gaussian convolution filter window of size 0.4 μm square. The theoretical resolution of 3PE microscopy at 700 nm (without smoothing) is <200 nm in the radial directions and ~500 nm in the axial direction (reported as the FWHM of the point spread function). Because of the longer wavelengths used, this is ~10% larger than the resolution obtained with the corresponding two-photon excitation (λ = 467 nm) and ~50% larger than the corresponding one-photon excitation (λ = 233 nm). However, for a given λ, the fundamental excitation focal volume, which better reflects the useful resolutions [J. Mertz, C. Xu, W. W. Webb, *Opt. Lett.* **20**, 2532 (1995)], is significantly smaller for 3PE. RBL cells were grown and harvested as described [J. L. Thomas *et al.*, *J. Cell Biol.* **125**, 795 (1994)]. Serotonin (Sigma) in aqueous solution (250 μM) was added 6 hours before imaging. The excitation pulses were pre-chirped by a double pass through an SF-10 prism pair to compensate for the dispersion caused by other optical elements (J. B. Guild, C. Xu, W. W. Webb, *Appl. Opt.*, in press). The pre-chirped light was directed into a confocal scanner (MRC 600, Bio-Rad; with optics modified for infrared reflection) and then onto an inverted microscope (Zeiss IM-35) containing a Zeiss Neofluar 63×/1.25 NA oil immersion objective lens. The input optics of the microscope were replaced by optics capable of simultaneous UV and infrared reflectance (Bio-Rad). The focused excitation beam optically scanned the specimen in the horizontal plane, and the specimen was stepped in the vertical direction, resulting in a series of "optical slices" that could be computer-reconstructed into a three-dimensional image. To avoid signal loss inside the scanner, we separated the epi-collected fluorescence from the excitation light before the scanner by a UV reflecting dichroic mirror (Omega), filtered with two 340 ± 20 nm interference filters (Barr Associates) and a 2-mm colored glass filter (UG11, Schott, the combined filter transmission is 0.22 at 350 nm and $<10^{-9}$ above 400 nm) and detected with a photomultiplier tube–amplifier module (HC125-02, Hamamatsu).
19. This work was carried out in the Developmental Resource for Biophysical Imaging and Optoelectronics with funding provided by NSF (grant DIR8800278) and NIH (grants RR07719 and RR04224). We gratefully acknowledge the NIH Parallel Processing Resource for Biomedical Scientists and the use of the IBM SP2 supercomputer at the Cornell Theory Center. We also thank Coherent and Spectra-Physics for loaning us Ti:sapphire mode-locked laser systems. J.B.S. is an NSF postdoctoral fellow.

12 August 1996; accepted 15 November 1996